

Supporting Information

Regulating Force-resistance and Acid-responsiveness of Purely Organics with Persistent Phosphorescence via Simple Isomerization

Yan Liu,^{ad} Zhimin Ma,^{bd} Xin Cheng,^a Chen Qian,^a Jianwei Liu,^a Xue Zhang,^a Mingxing Chen,^c Xinru Jia^c and Zhiyong Ma^{a}*

^a Beijing State Key Laboratory of Organic-Inorganic Composites, College of Chemical Engineering, Beijing University of Chemical Technology, Beijing 100029, China. E-mail: mazhy@mail.buct.edu.cn

^b National high-tech industrial development zone in Jingdezhen, Jingdezhen, 333000, China.

^c Beijing National Laboratory for Molecular Sciences, Key Laboratory of Polymer Chemistry and Physics of the Ministry of Education, College of Chemistry and Molecular Engineering, Peking University, Beijing 100871, China.

^d These authors contributed equally to this work.

1. Materials and General Methods

All the solvents and reactants were purchased from commercialized companies and used as received without further purification except for specifying otherwise.

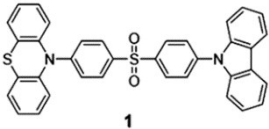
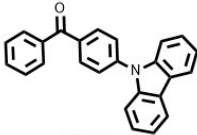
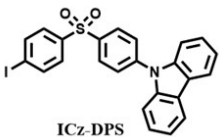
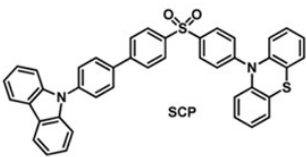
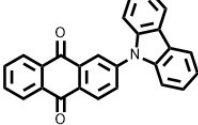
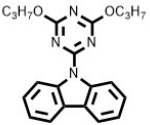
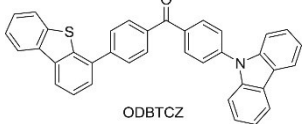
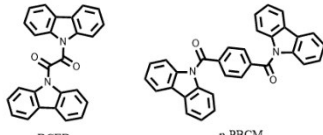
^1H NMR was recorded on the 400 MHz (Bruker ARX400) and ^{13}C NMR spectra were recorded on the Bruker 101 MHz spectrometer at room temperature with CDCl_3 as the solvent and tetramethylsilane (TMS) as the internal standard. ESI high resolution mass-spectra (HRMS) were acquired on a Bruker Apex IV FTMS mass spectrometer. UV-Vis spectra were acquired on the Hitachi U-3900H UV-vis spectrophotometer. Transient and delayed photoluminescence spectra were performed on the Hitachi F-7000 or Edinburgh Instruments FLS980 fluorescence spectrophotometer equipped with a continuous xenon lamp (Xe1) and a microsecond flashlamp, respectively. Phosphorescence lifetime were acquired on the Edinburgh Instruments FLS980 fluorescence spectrophotometer ($\lambda_{\text{ex}}=365$ nm) equipped with a microsecond flashlamp. The emission lifetime of the samples was determined by the Time Correlated Single Photon Counting (TCSPC) technique using an Edinburgh Instruments mini-tau lifetime spectrophotometer equipped with an EPL 375 pulsed diode laser. Differential scanning calorimetry (DSC) measurement was carried out by using TA instruments Q100 DSC. Wide-angle X-ray diffraction (WAXD) experiments were performed on a Philips X'PertPro diffractometer with a 3 kW ceramic tube as the X-ray source ($\text{Cu K}\alpha$) and an X'celerator detector. Single crystal X-ray diffraction data were collected with a NONIUS KappaCCD diffractometer with graphite monochromator and $\text{Mo K}\alpha$ radiation [λ ($\text{MoK}\alpha$) = 0.71073 Å]. Structures were solved by direct methods with SHELXS-97 and refined against F2 with SHELXS-97.

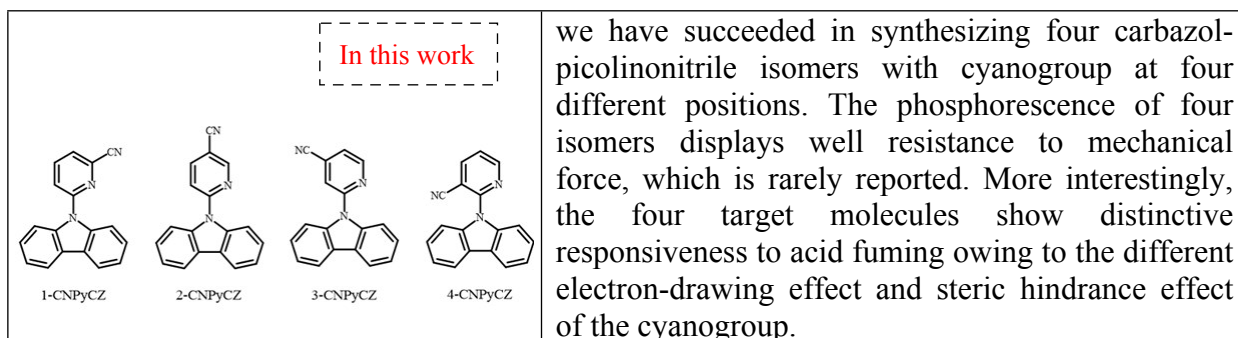
Photoluminescence and phosphorescence quantum yield measurements were conducted in F-3018 integrating sphere setup from Horiba Scientific, connected to and operated from a Fluorolog

fluorometer also from Horiba Scientific. The data analysis was executed with the software included with the F-3018 integrating sphere. In order to eliminate the influence of short-lived fluorescence, the phosphorescent quantum yield test light source uses a pulsed xenon lamp with a pulse frequency of 5 Hz and a delay time of 50 μ s.

TD-DFT calculations were conducted on Gaussian 09 program with a method similar to previous literature.¹ Ground state (S_0) geometries of **4-CNPyCZ** were directly selected from single crystal structures and were used as molecular models without further optimization. On the basis of this, exciton energies in singlet (S_n) and triplet states (T_n) were estimated through a combination of TDDFT and B3LYP at the 6-311+G(d,p) level. Kohn-Sham frontier orbital analysis was subsequently performed based on the results of theoretical calculation to elucidate the mechanisms of possible singlet-triplet intersystem crossings, in which the channels from S_1 to T_n are believed to share part of the same transition orbital compositions. Herein, energy levels of the possible T_n states are considered to lie within the range of $ES_1 \pm 0.3$ eV.²

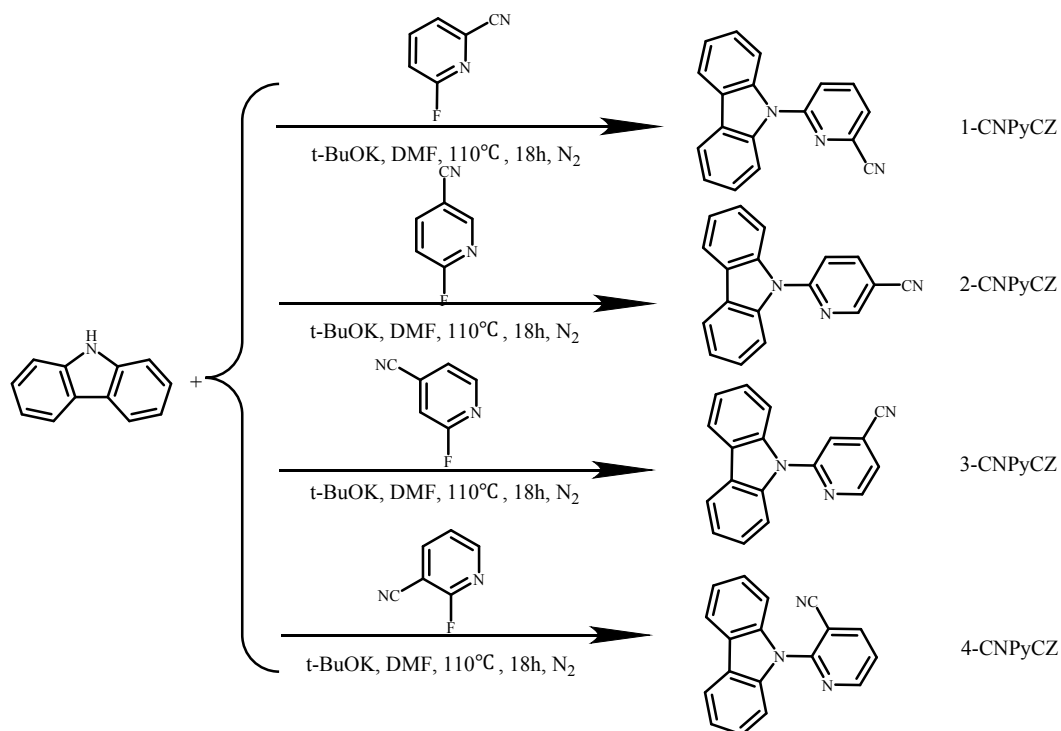
2. Background Information

Molecular structure	main content
 <p style="text-align: center;">1</p> <p>Angew.Chem. Int.Ed, 54(3), 874-878; 2015</p>	<p>Compound 1 is a novel AIE-DF material with asymmetric structure. Simultaneously, 1 exhibited strong ML (bright green light) without any pretreatment.</p>
 <p style="text-align: center;">CzBP</p> <p>Advanced Materials, 2015, 27(40): 6195-6201.</p>	<p>CZBP molecules exhibit transient fluorescence, delayed fluorescence and phosphorescence. After grinding, the bright white luminescence of CzBP becomes dark blue due to the disappearance of the continuous emission of yellow. Through heat treatment or solvent fumigation, the luminous color of the ground powder can be completely restored to the original state.</p>
 <p style="text-align: center;">ICz-DPS</p> <p>Angew.Chem. Int.Ed, 2015, 54(21): 6270-6273.</p>	<p>Compound ICz-DPS exhibit excellent room-temperature fluorescent-phosphorescent dual-emission (rFPDE) properties. The novel rFPDE compound ICz - DPS can realize white emission by proper external mechanical stimuli, fitting with the principle of color mixing.</p>
 <p style="text-align: center;">SCP</p> <p>Chem. Sci., 2016,7, 2201-2206</p>	<p>Compound SCP is a kind of molecule that can regulate white light emission by external grinding. This is because the bright white light emission can be obtained when conventional fluorescence and thermal activation delayed fluorescence (TADF) are combined in a certain proportion during grinding process.</p>
 <p style="text-align: center;">Cz-AQ</p> <p>J. Mater. Chem. C, 2017,5, 12031-12034</p>	<p>Compound Cz-AQ is an AIE-TADF material, which exhibited reversible ML. On the basis of single-crystal structural study, indicating that enhanced π-π interaction induced the shift in fluorescence emission from yellow to red.</p>
 <p style="text-align: center;">PCzT</p> <p>Angew.Chem. Int.Ed. 2018, 57,8425 -8431</p>	<p>Upon prolonged photoirradiation, the UOP of Compound PCzT could be activated, achieving dynamic and reversible ultralong organic phosphorescence by manipulating intermolecular interactions in the crystalline state with external stimuli.</p>
 <p style="text-align: center;">ODBTCZ</p> <p>Dyes and Pigments, 2019, 173:107963.</p>	<p>ODBTCZ is a rarely reported pure organic RTP molecule with dual-mode mechanochromism including fluorescence redshift and RTP/DF on-off switch.</p>
 <p style="text-align: center;">DCED p-PBCM</p> <p>Adv. Mater. 2019, 31, 1807222</p>	<p>After grinding, the phosphorescence of molecule DCED disappeared. However, the phosphorescence of molecule p-PBCM retains even suffered from vigorous mechanical grinding, which is rarely found for pure organics.</p>



The reported Stimulus-responsive luminescent material based on carbazole group.³⁻¹⁰

3. Synthetic route to 1-CNPyCZ, 2-CNPyCZ, 3-CNPyCZ and 4-CNPyCZ.



Scheme S1. The synthetic routes to 1-CNPyCZ, 2-CNPyCZ, 3-CNPyCZ and 4-CNPyCZ .

Synthesis of 1-CNPyCZ: t-BuOK (961 mg, 8.56 mmol) was added to a 100 mL schlenk flask; then 10 mL DMF (AR grade) was injected under nitrogen atmosphere. After the mixture was stirred at room temperature for 15 min, carbazole (836.1 mg, 5 mmol) dissolved in 10 ml DMF (AR grade) was carefully added and the resultant solution was stirred at room temperature for 3 h. Then 2-Cyano-6-Fluoropyridine (610.5 mg, 5 mmol) dissolved in 10 ml DMF (AR grade) was carefully added and the resultant solution was stirred at 110 °C for 18 h. After the reaction was over, the resultant mixture was cooled down to room temperature and the solvent was removed under reduced pressure. The crude product was purified by column chromatography using ethyl acetate and petroleum ether (v/v, 1:6) as the eluent to obtain pure product as white powder in 26% yield (350.6 mg). ¹H NMR (400 MHz, CDCl₃) δ =8.16-8.05 (m, 2H), 8.00-7.84 (m, 4H), 7.61 (d, J =7.4 Hz, 1H), 7.51-7.44 (m, 2H), 7.41-7.33 (m, 2H). ¹³C NMR (101 MHz, CDCl₃) δ 153.05 (s), 139.47 (s), 138.88 (s), 133.21 (s), 126.65 (s), 125.20 (s), 124.91 (s), 122.03 (s), 121.79 (s), 120.37 (s),

116.81 (s), 111.44 (s). HR-ESI-MS Calcd. For $C_{18}H_{11}N_3$ $[M+H]^+$: 270.102574. Found: 270.102503.

Synthesis of 2-CNPyCZ: Following the similar synthesis of 1-CNPyCZ, 2-CNPyCZ was obtained as white powder by using 5-Cyano-2-fluoropyridine in place of 2-Cyano-6-Fluoropyridine. Yield: 33% (440.8 mg). 1H NMR (400 MHz, $CDCl_3$) δ = 8.91 (d, J = 2.3 Hz, 1H), 8.12 – 8.09 (m, 2H), 8.05 (dd, J = 8.6, 2.3 Hz, 1H), 7.96 (d, J = 8.3 Hz, 2H), 7.75 (d, J = 8.6 Hz, 1H), 7.47 (ddd, J = 8.4, 7.2, 1.3 Hz, 2H), 7.38 (td, J = 7.5, 1.0 Hz, 2H). ^{13}C NMR (101 MHz, Chloroform- d) δ 154.60 (s), 152.80 (s), 141.25 (s), 138.78 (s), 126.74 (s), 125.28 (s), 122.40 (s), 120.42 (s), 117.47 (s), 116.69 (s), 111.93 (s), 105.69 (s). HR-ESI-MS Calcd. For $C_{18}H_{11}N_3$ $[M+H]^+$: 270.102574. Found: 270.102774.

Synthesis of 3-CNPyCZ: Following the similar synthesis of 1-CNPyCZ, 3-CNPyCZ was obtained as white powder by using 4-Cyano-2-fluoropyridine in place of 2-Cyano-6-Fluoropyridine. Yield: 37% (500.5 mg). 1H NMR (400 MHz, Chloroform- d) δ 8.86 (dd, J = 5.0, 0.9 Hz, 1H), 8.13 – 8.10 (m, 2H), 7.91 – 7.87 (m, 3H), 7.50 – 7.45 (m, 3H), 7.37 (td, J = 7.5, 1.0 Hz, 2H). ^{13}C NMR (101 MHz, Chloroform- d) δ 152.94 (s), 150.78 (s), 138.92 (s), 126.67 (s), 124.90 (s), 122.67 (s), 122.04 (s), 121.67 (s), 120.44 (s), 120.02 (s), 116.17 (s), 111.22 (s). HR-ESI-MS Calcd. For $C_{18}H_{11}N_3$ $[M+H]^+$: 270.102574. Found: 270.102755.

Synthesis of 4-CNPyCZ: Following the similar synthesis of 1-CNPyCZ, 4-CNPyCZ was obtained as white powder by using 3-Cyano-2-fluoropyridine in place of 2-Cyano-6-Fluoropyridine. Yield: 33% (450.6 mg). 1H NMR (400 MHz, Chloroform- d) δ 8.89 (dd, J = 4.9, 1.9 Hz, 1H), 8.24 (dd, J = 7.8, 2.0 Hz, 1H), 8.16 – 8.12 (m, 2H), 7.49 – 7.45 (m, 5H), 7.37 (ddd, J = 8.0, 5.0, 3.2 Hz, 2H). ^{13}C NMR (101 MHz, Chloroform- d) δ 153.37 (s), 143.43 (s), 139.43 (s), 126.28 (s), 124.66 (s), 121.90 (s), 121.80 (s), 120.51 (s), 115.06 (s), 110.95 (s), 106.87 (s). HR-ESI-MS Calcd. For $C_{18}H_{11}N_3$ $[M+H]^+$: 270.102574. Found: 270.102557.

Figure S4. ^1H NMR spectrum of 2-CNPyCZ in CDCl_3 .

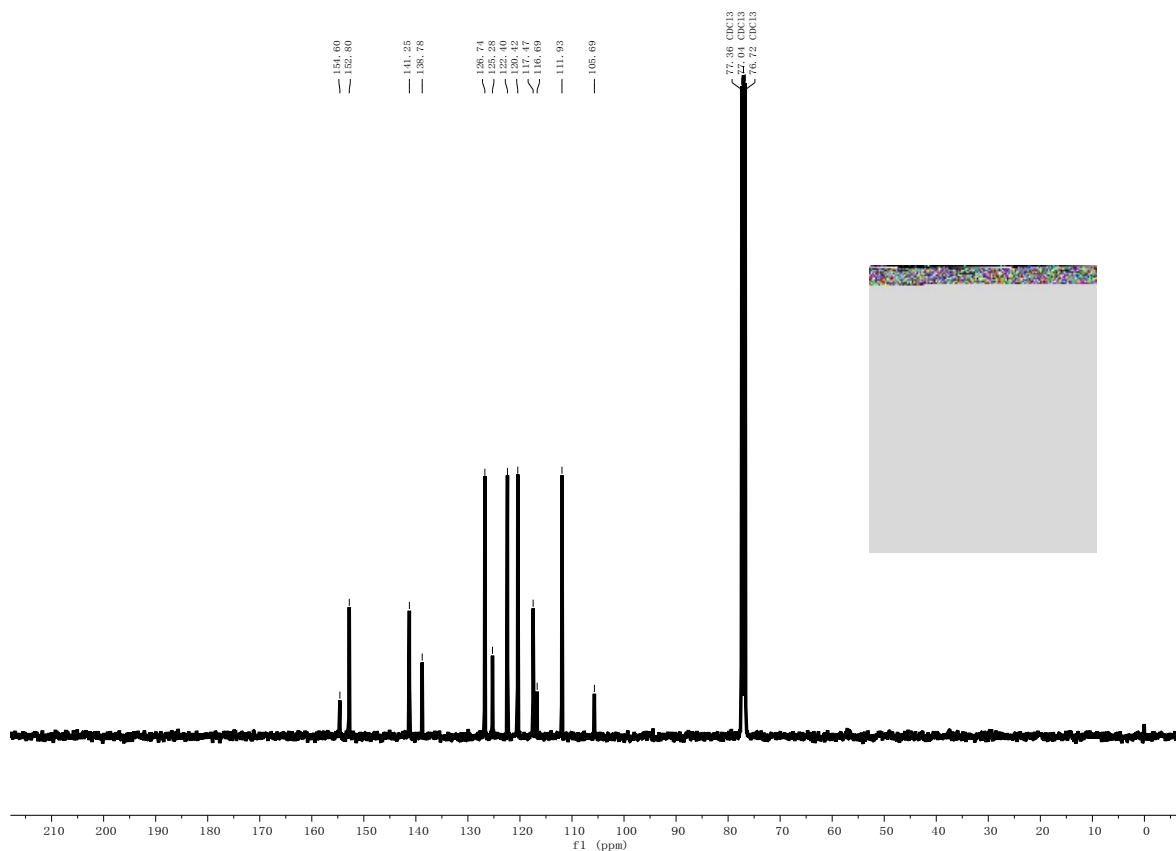


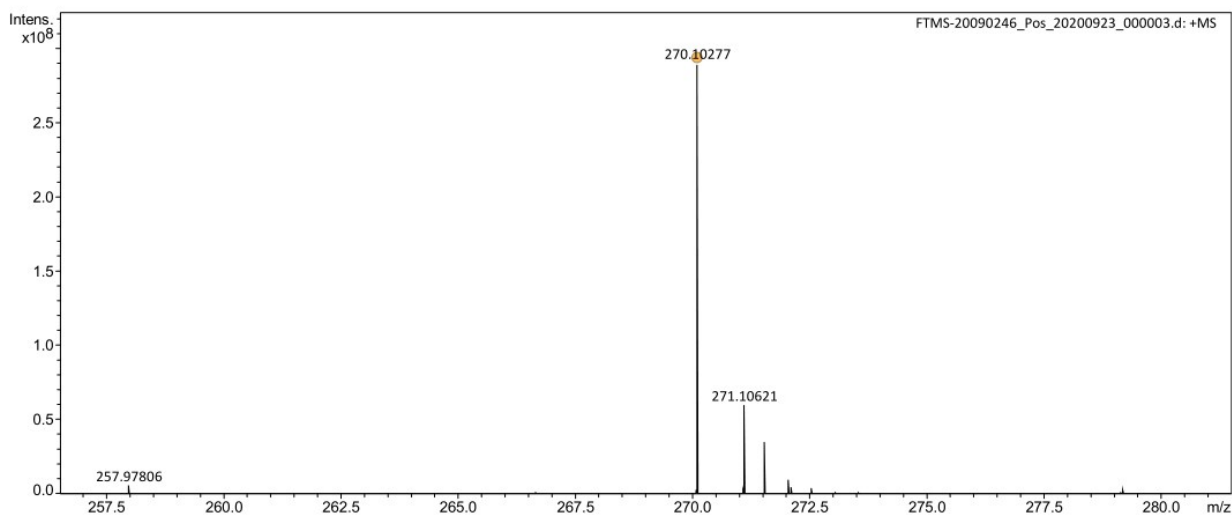
Figure S5. ^{13}C NMR spectrum of 2-CNPyCZ in CDCl_3 .

Peking University Mass Spectrometry Sample Analysis Report

Analysis Info

Analysis Name FTMS-20090246_Pos_20200923_000003.d
Sample 2-CNPyCZ
Comment

Acquisition Date 9/23/2020 4:11:01 PM
Instrument Bruker Solarix XR FTMS
Operator Peking University



Meas. m/z	#	Ion Formula	Score	m/z	err [ppm]	Mean err [ppm]	mSigma	rdb	e ⁻ Conf	N-Rule
270.102774	1	C18H12N3	100.00	270.102574	-0.7	-1.3	6.0	15.0	even	ok

Figure S6. HR-MS spectrum of 2-CNPyCZ.

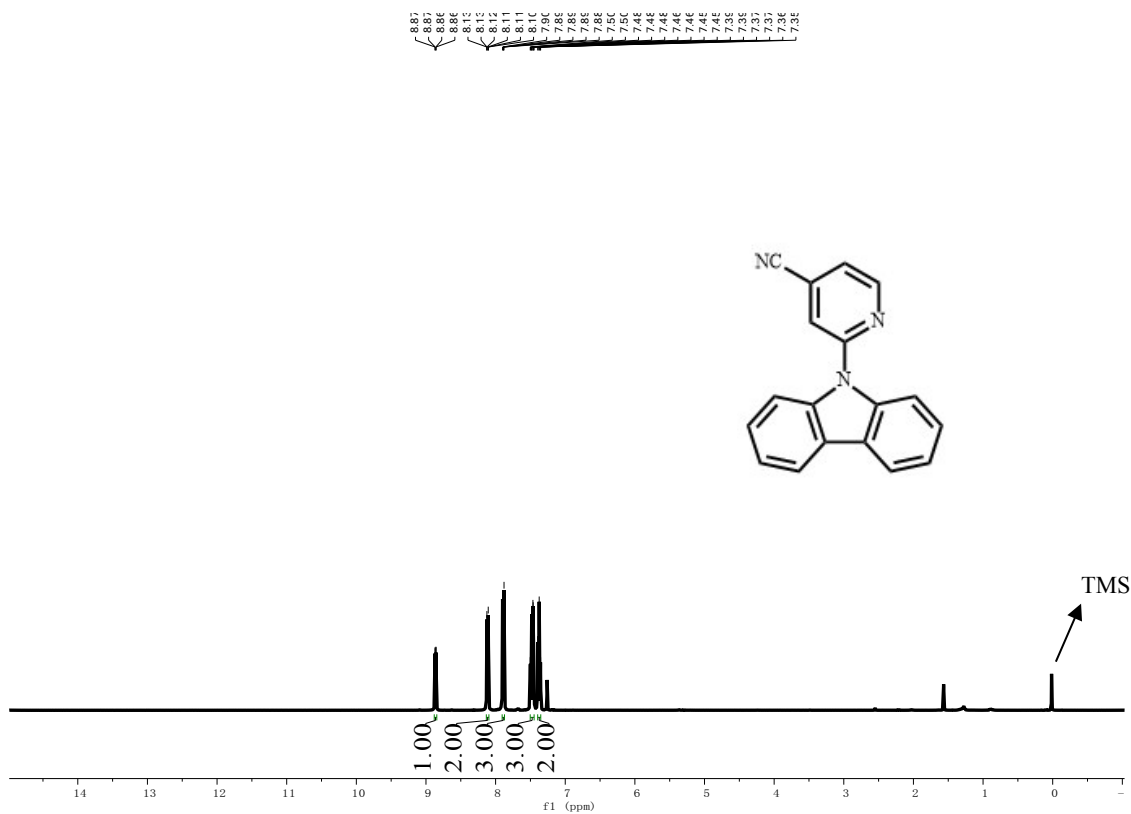


Figure S7. ^1H NMR spectrum of 3-CNPyCZ in CDCl_3 .

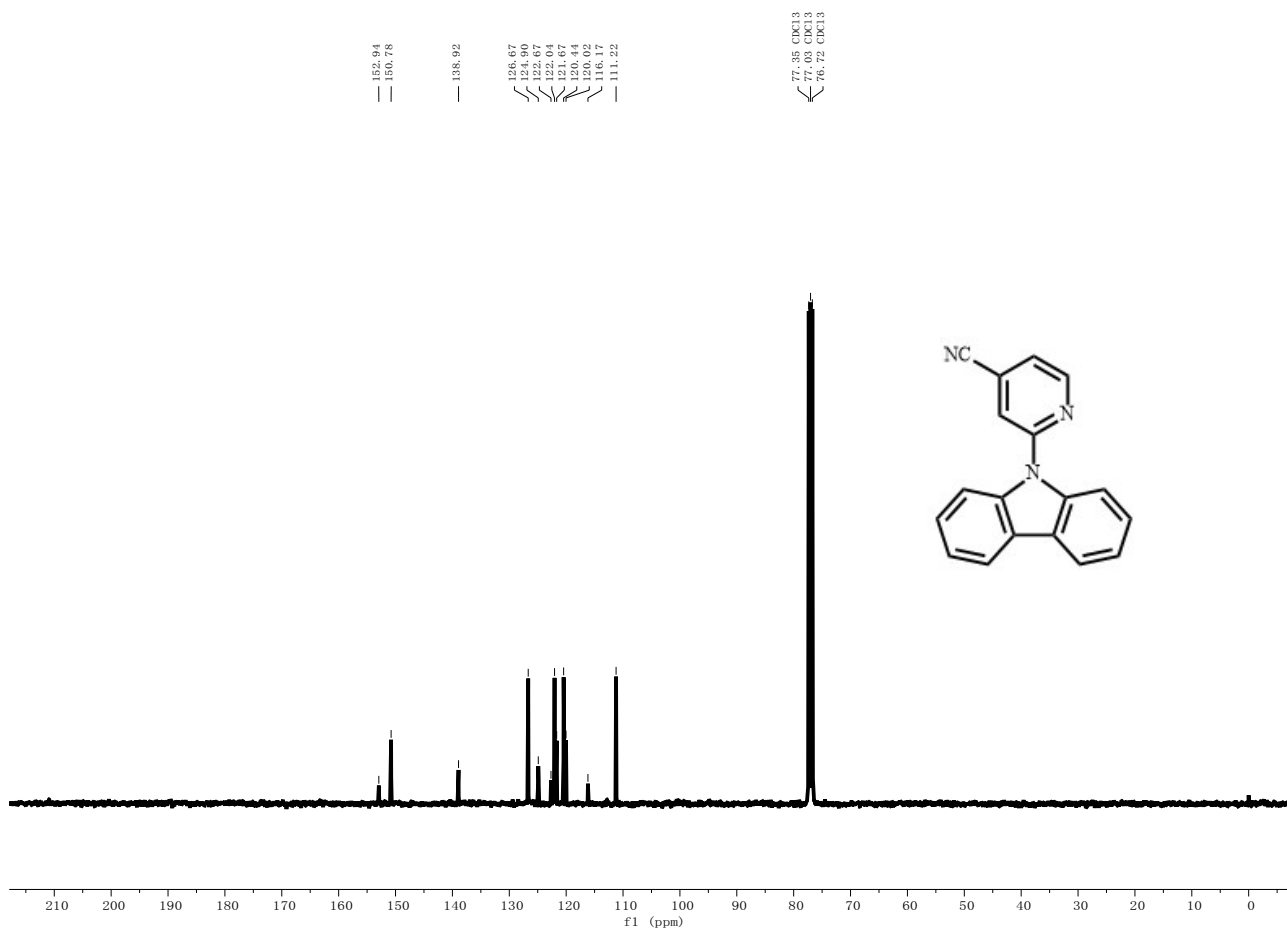


Figure S8. ^{13}C NMR spectrum of 3-CNPyCZ in CDCl_3 .

Peking University Mass Spectrometry Sample Analysis Report

Analysis Info

Analysis Name FTMS-20090246_Pos_20200923_000005.d
 Sample 3-CNPyCZ
 Comment

Acquisition Date 9/23/2020 4:14:05 PM
 Instrument Bruker Solarix XR FTMS
 Operator Peking University

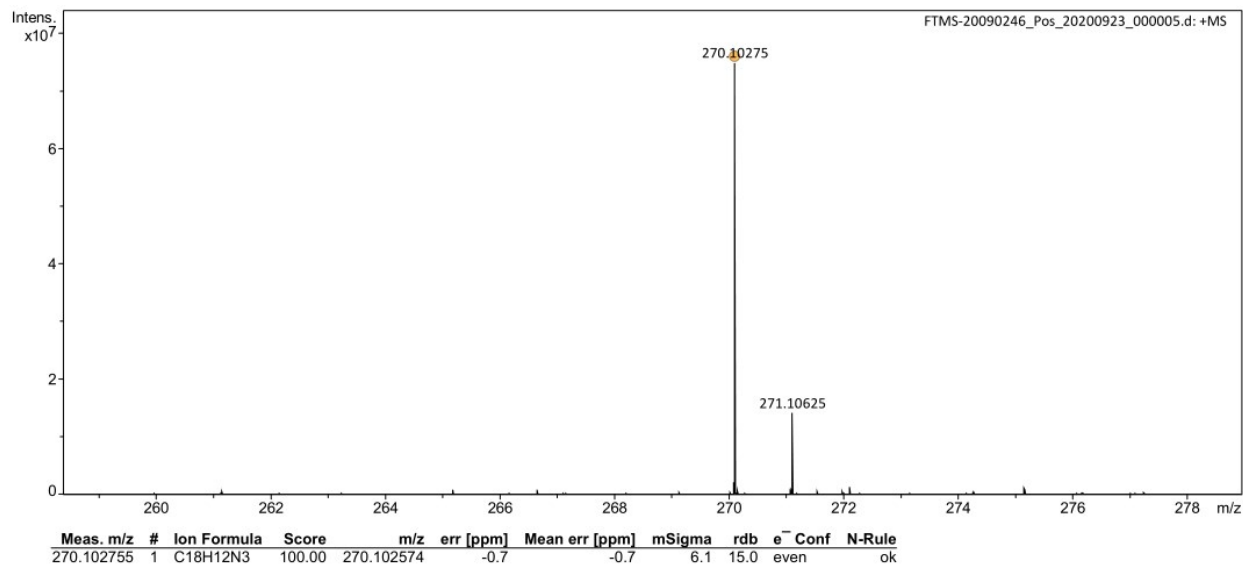


Figure S9. HR-MS spectrum of **3-CNPyCZ**.

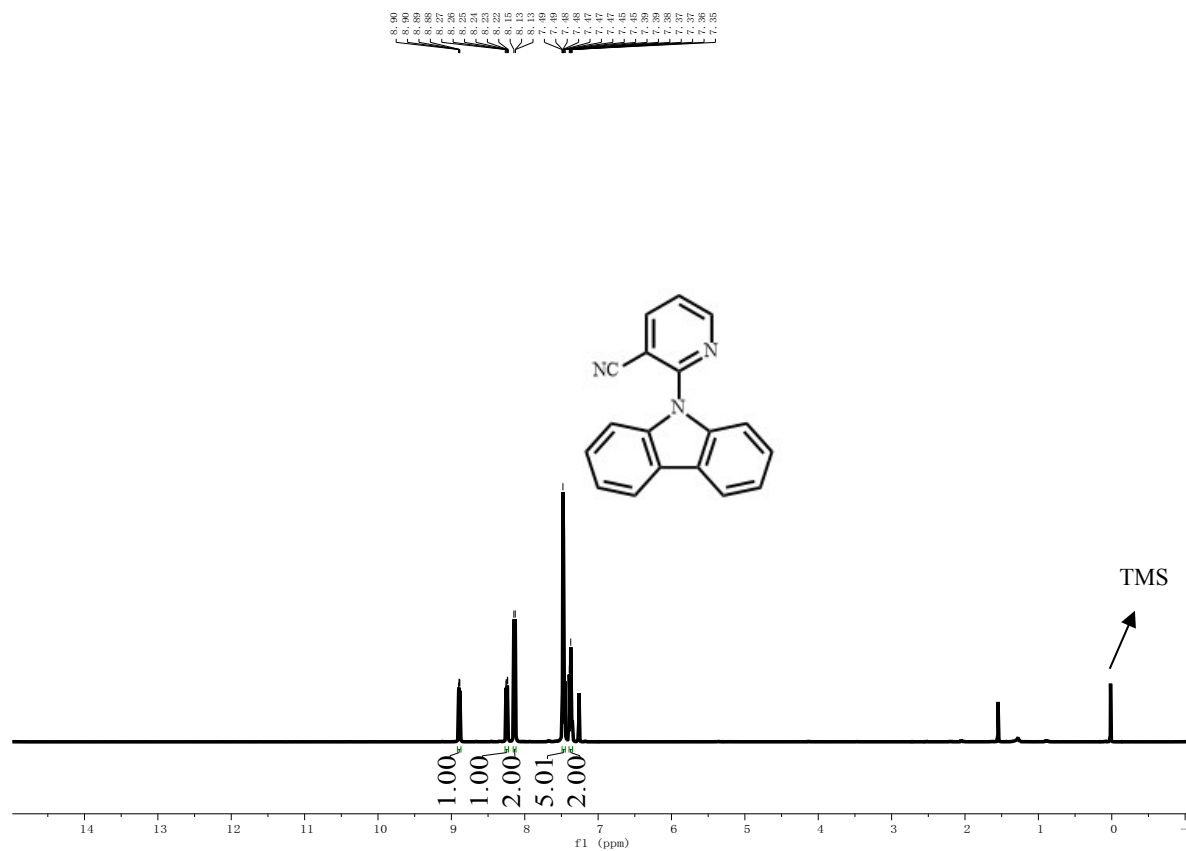


Figure S10. ¹H NMR spectrum of **4-CNPyCZ** in CDCl₃.

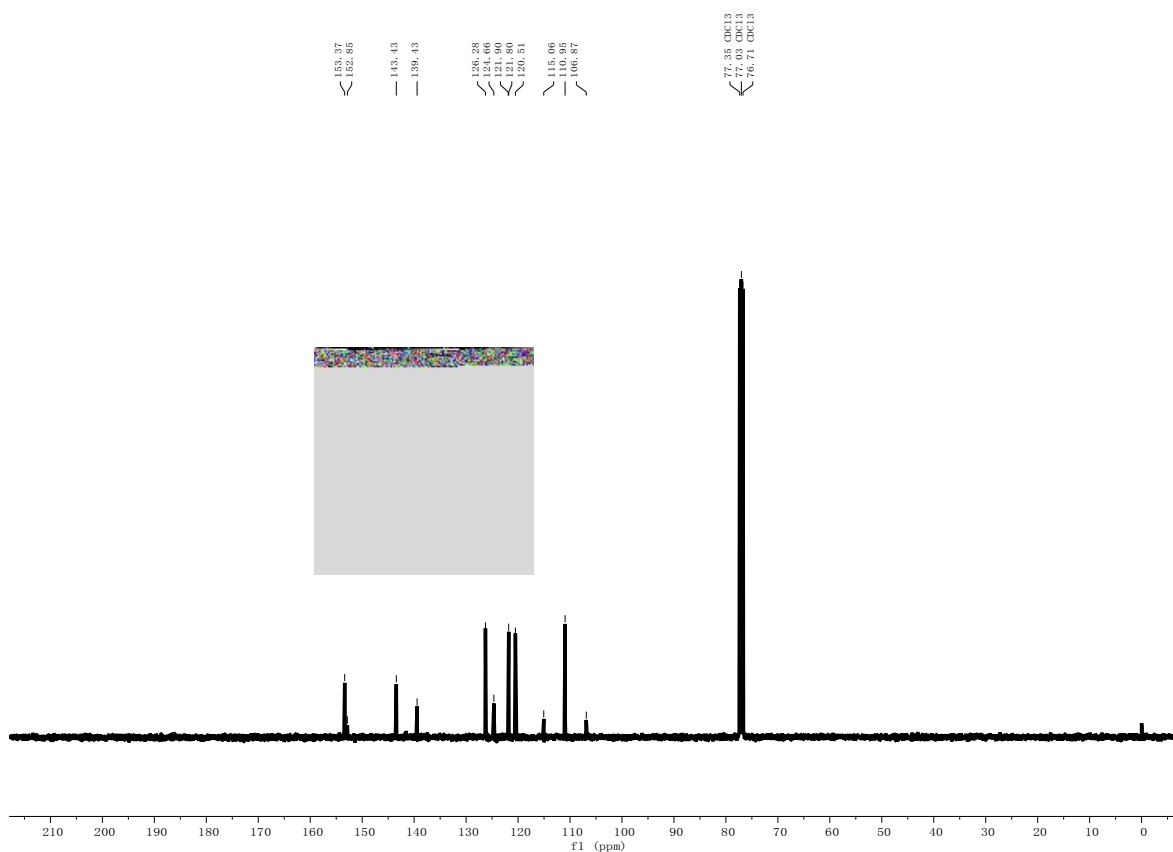


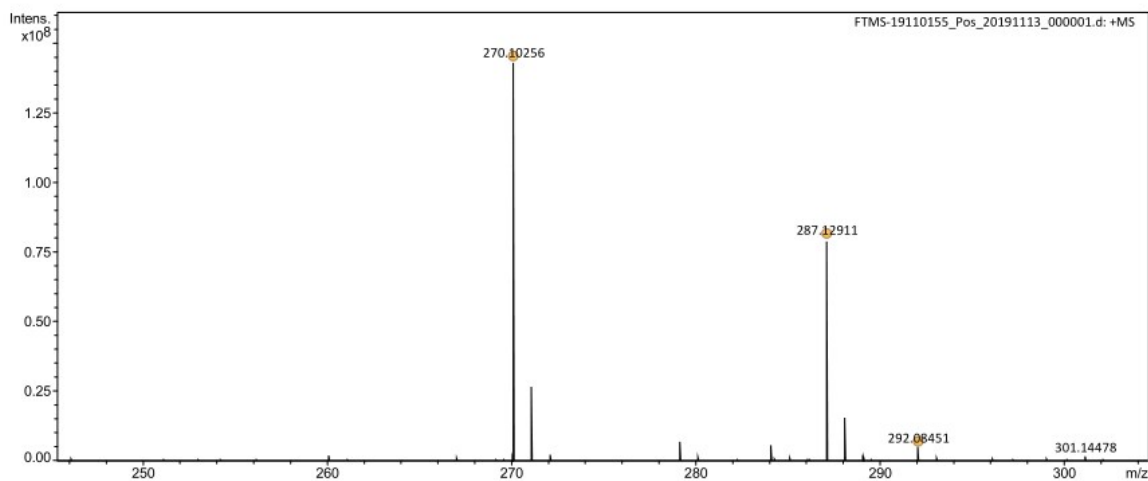
Figure S11. ^{13}C NMR spectrum of 4-CNPyCZ in CDCl_3 .

Peking University Mass Spectrometry Sample Analysis Report

Analysis Info

Analysis Name FTMS-19110155_Pos_20191113_000001.d
 Sample 4-1
 Comment

Acquisition Date 11/13/2019 3:51:28 PM
 Instrument Bruker Solarix XR FTMS
 Operator Peking University



Meas. m/z	#	Ion Formula	Score	m/z	err [ppm]	Mean err [ppm]	mSigma	rdb	e ⁻ Conf	N-Rule
270.10257	1	C ₁₈ H ₁₂ N ₃	100.00	270.102574	0.1	-0.1	3.9	15.0	even	ok
287.129109	1	C ₁₈ H ₁₅ N ₄	100.00	287.129123	0.1	-0.1	0.6	14.0	even	ok
292.084507	1	C ₁₈ H ₁₁ N ₃ Na	100.00	292.084518	0.0	0.1	8.6	15.0	even	ok

Figure S12. HR-MS spectrum of 4-CNPyCZ.

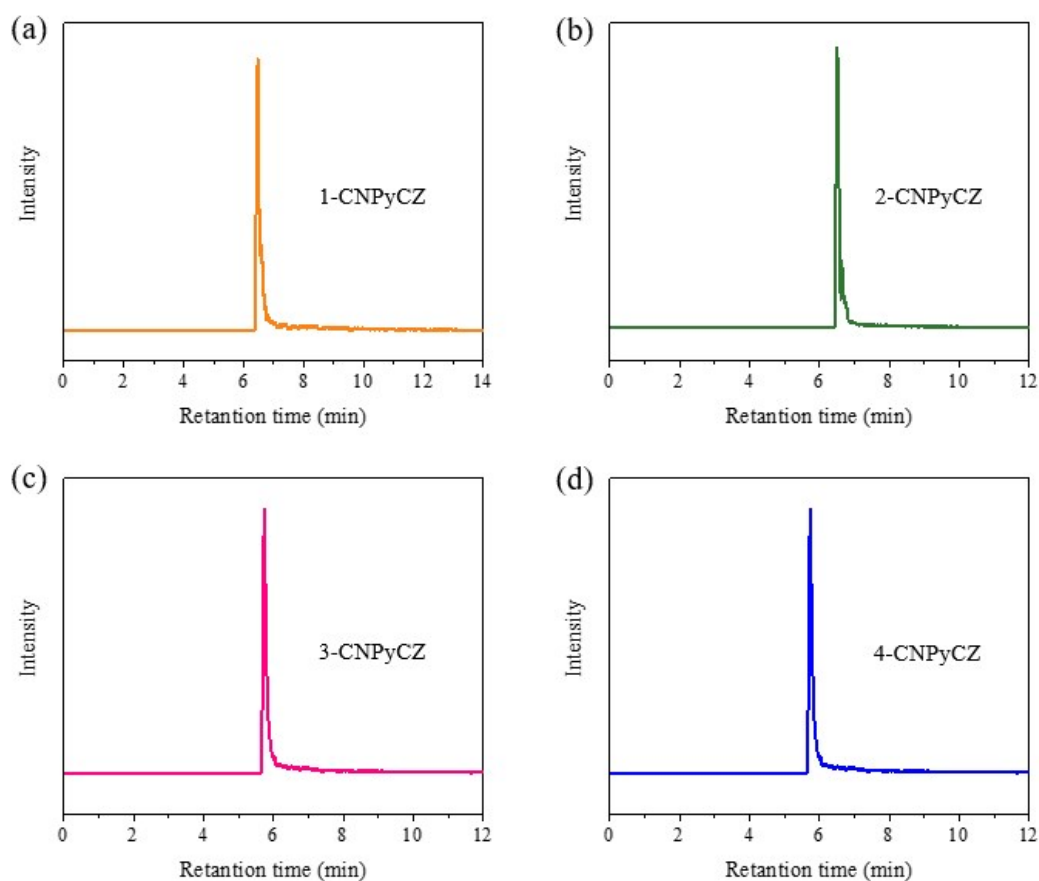


Figure S13. HPLC curves of (a) 1-CNPyCZ; (b) 2-CNPyCZ; (c) 3-CNPyCZ; (d) 4-CNPyCZ.

5. Data table of single crystal 1-CNPyCZ, 2-CNPyCZ and 4-CNPyCZ

Table S1. Detailed data of 1-CNPyCZ, 2-CNPyCZ and 4-CNPyCZ single crystals.

Identification code	1-CNPyCZ	2-CNPyCZ	4-CNPyCZ
CCDC Number	2048684	2048685	2048686
Empirical formula	$C_{18}H_{11}N_3$	$C_{18}H_{11}N_3$	$C_{18}H_{11}N_3$
Formula weight	269.30	269.30	269.30
Temperature	110 K	98 K	162 K
Wavelength	0.71073 Å	0.71073 Å	0.71073 Å
Crystal system	monoclinic	monoclinic	orthorhombic
Space group	$P 1 21/n 1$	$P2(1)/n$	$P b c a$
Unit cell dimensions	$a = 9.0032(3) \text{ \AA}, \alpha = 90.00^\circ$ $b = 7.3984(2) \text{ \AA}, \beta = 90.3690(10)^\circ$ $c = 20.0691(7) \text{ \AA}, \gamma = 90.00^\circ$	$a = 9.0308(3) \text{ \AA}, \alpha = 90.00^\circ$ $b = 7.5081(2) \text{ \AA}, \beta = 98.9470(10)^\circ$ $c = 20.1212(7) \text{ \AA}, \gamma = 90.00^\circ$	$a = 14.664(3) \text{ \AA}, \alpha = 90.00^\circ$ $b = 11.881(2) \text{ \AA}, \beta = 90.00^\circ$ $c = 15.315(3) \text{ \AA}, \gamma = 90.00^\circ$
Volume	1336.76 \AA^3	1347.70 \AA^3	2668.2 \AA^3

Z	4	4	8
Density (calculated)	1.338 mg/mm ³	1.327 mg/mm ³	1.341 mg/mm ³
Absorption coefficient	0.082 mm ⁻¹	0.081 mm ⁻¹	0.082 mm ⁻¹
F(000)	560	560	1120
Crystal size	No data	0.15 x 0.18 x 0.25 mm ³	0.18 x 0.16 x 0.1 mm ³
Theta range for data collection	2.93 to 27.08°.	2.918 to 28.363°.	1.3887 to 27.4816°.
Index ranges	-11<=h<=11, -9<=k<=9, -25<=l<=25	-11<=h<=11, -9<=k<=9, -25<=l<=25	-17<=h<=17, -14<=k<=13, -18<=l<=18
Reflections collected	2946	2866	2343
Independent reflections	2449 [R(int) = 0.0430]	2306 [R(int) = 0.0374]	2307[R(int) = 0.0511]
Final R indices [I>2sigma(I)]	R1 =0.0409, wR2 =0.0934	R1 =0.0425, wR2 =0.1056	R1 =0.0566, wR2 =0.1174
R indices (all data)	R1 = 0.0508, wR2 = 0.1017	R1 = 0.0549, wR2 = 0.0.1187	R1 = 0.0581, wR2 = 0.1166

6. Photophysical properties of 1-CNPyCZ, 2-CNPyCZ, 3-CNPyCZ and 4-CNPyCZ

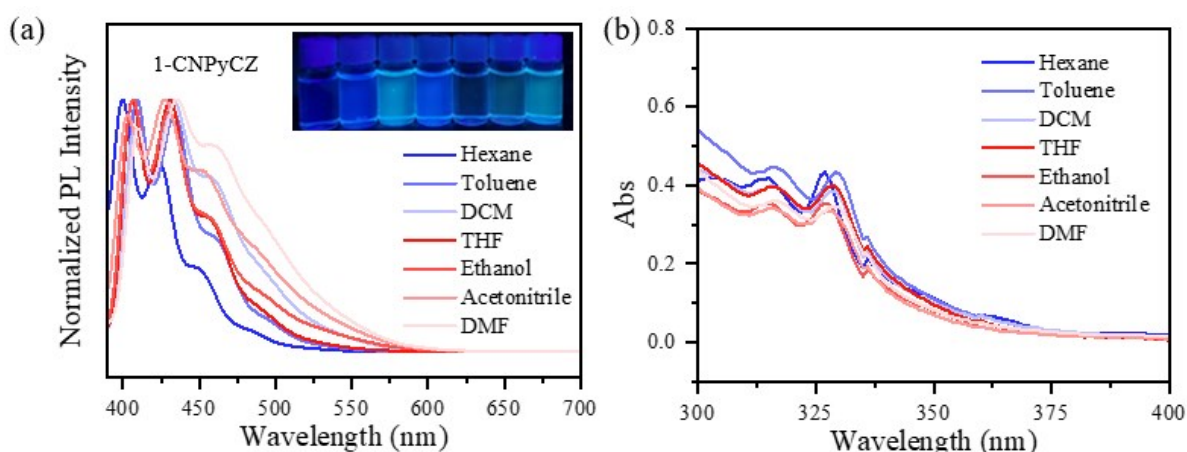


Figure S14. (a) Fluorescence spectra (inset: fluorescent images of **1-CNPyCZ** in different organic solvent under 365 nm UV light), (b) absorption spectra of **1-CNPyCZ** (20 μM) in different organic solvent.

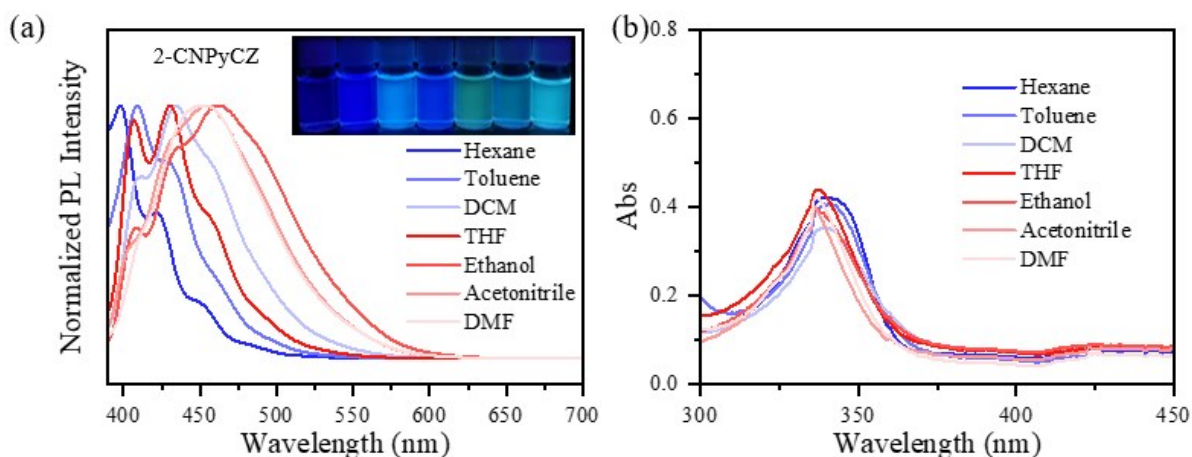


Figure S15. (a) Fluorescence spectra (inset: fluorescent images of **2-CNPyCZ** in different organic solvent under 365 nm UV light), (b) absorption spectra of **2-CNPyCZ** (20 μM) in different organic solvent.

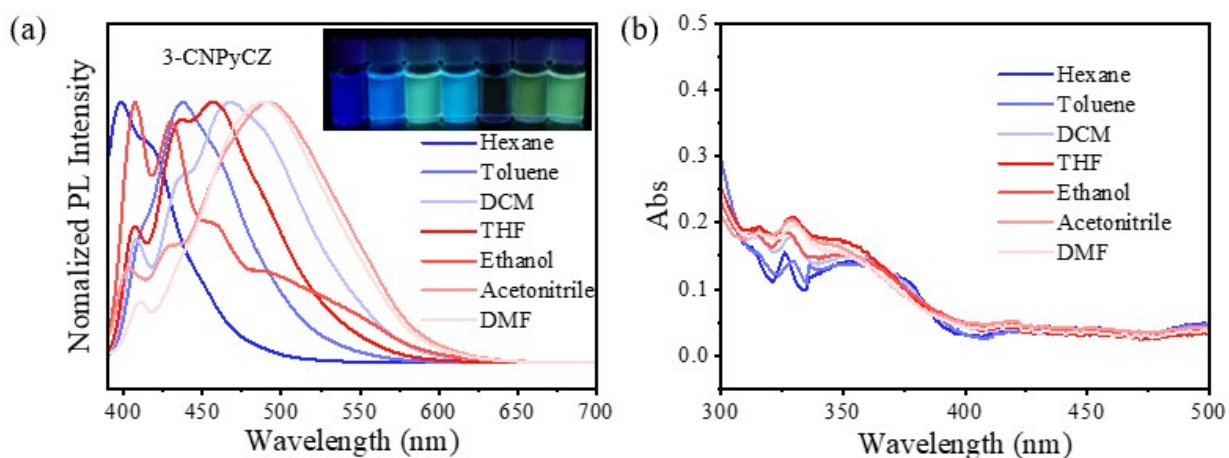


Figure S16. (a) Fluorescence spectra (inset: fluorescent images of **3-CNPyCZ** in different organic solvent under 365 nm UV light), (b) absorption spectra of **3-CNPyCZ** (20 μM) in different organic solvent.

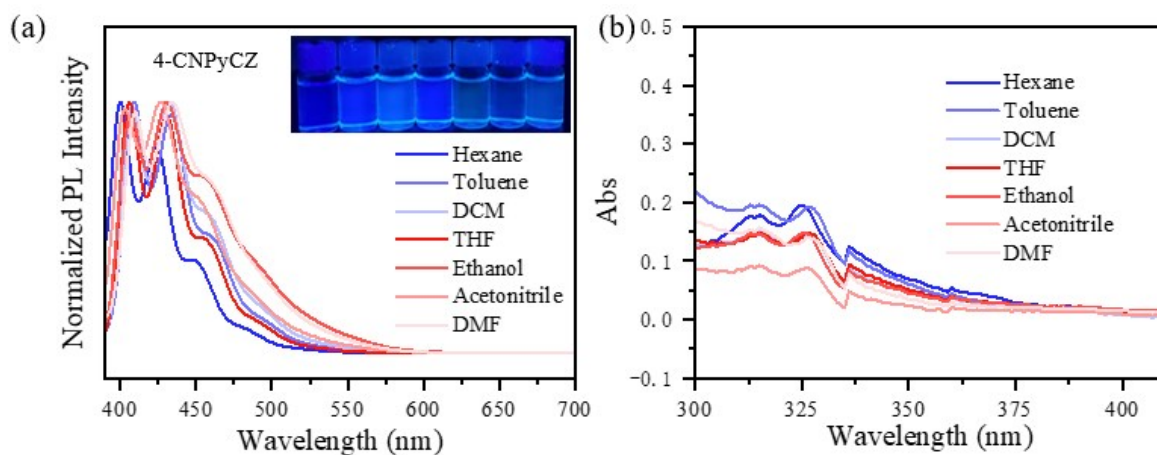


Figure S17. (a) Fluorescence spectra (inset: fluorescent images of 4-CNPyCZ in different organic solvent under 365 nm UV light), (b) absorption spectra of 4-CNPyCZ (20 μM) in different organic solvent.

7. HOMO and LUMO

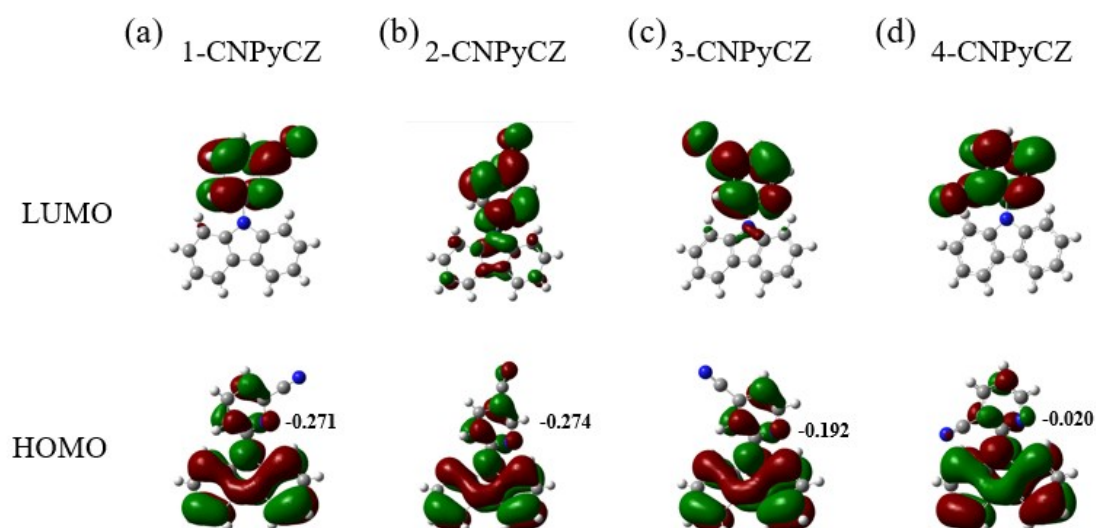


Figure S18. The HOMO and LUMO of the single molecule in the 1-CNPyCZ, 2-CNPyCZ, 3-CNPyCZ and 4-CNPyCZ. The data is Mulliken charge distribution of nitrogen atom in the pyridine ring.

8. Summary of photophysical parameters of 1-CNPyCZ, 2-CNPyCZ, 3-CNPyCZ and 4-CNPyCZ

Table S2. Photophysical properties of 1-CNPyCZ, 2-CNPyCZ, 3-CNPyCZ and 4-CNPyCZ in different states.

sample	Fluorescence								Phosphorescence			
	λ^a /nm	τ_F^a /ns	λ^b /nm	τ_F^b /ns	λ^c /nm	τ_F^c /ns	λ^d /nm	τ_F^d /ns	λ^a /nm	τ_P^a /ms	λ^b /nm	τ_P^b /s
1-CNPyCZ	410	10.00	455	32.94	-	-	-	-	555	543.55	474	0.55
			480	35.63					600	543.14		
			513	35.22								
2-CNPyCZ	423	5.07	405	6.32	-	-	485	3.68	432	199.66	425	0.35
			422	6.98					550	640.39		
									590	658.93		
3-CNPyCZ	432	8.78	455	15.98	-	-	570	2.27	547	643.62	455	0.18
									595	617.55		
									650	625.89		
4-CNPyCZ	401	11.62	401	17.07	414	10.45	401	13.65	500	25.35	440	1.79
	525	15.23	416	17.97			525	18.65	550	544.77		
							600	587.92	600	587.92		

^a original powder at 298 K; ^b doped film (1 wt%) at 77 K; ^c ground powder at 298 K; ^d fumed powder at 298 K.

Table S3. Photophysical properties of 1-CNPyCZ, 2-CNPyCZ, 3-CNPyCZ and 4-CNPyCZ in crystalline powder at room temperature.

sample	λ_{em} /nm	Fluorescence				Phosphorescence					
		τ_F /ns	Φ_F /%	$k_{rf}/10^7 S^{-1}$	$k_{nrf}/10^7 S^{-1}$	λ_p /nm	τ_P /ms	Φ_P /%	k_{rp}/S^{-1}	k_{nrp}/S^{-1}	$k_{ISC}/10^7 S^{-1}$
1-CNPyCZ	410	10	18.8	1.88	5.52	555	543.55	26.0	0.48	1.36	2.6
						600	543.14				
2-CNPyCZ	423	5.07	75.8	14.95	1.62	432	199.66	16.0	0.25	1.31	3.16
						550	640.39				
						590	658.93				
3-CNPyCZ	432	8.78	65.8	7.49	1.62	547	643.62	20.0	0.31	1.24	2.28
						595	617.55				
						650	625.89				
4-CNPyCZ	401	11.62	13.3	1.14	5.13	500	25.35	27.1	0.50	1.34	2.33
	525	15.23				550	544.77				
						600	587.92				

Abbreviation: λ_{em} : fluorescence maximum; λ_p : phosphorescence maximum; τ_F : fluorescence lifetime; Φ_F : fluorescence quantum efficiency; τ_P : phosphorescence lifetime; Φ_P : phosphorescence quantum efficiency; k_{rf} : rate constant of fluorescence; k_{rp} : rate constant of phosphorescence; k_{nrf} : rate constant of nonradiative decay of fluorescence; k_{nrp} : rate constant of nonradiative decay of phosphorescence; k_{ISC} : rate constant of intersystem crossing from singlet to triplet states. $k_{rf} = \Phi_F / \tau_F$, $k_{rp} = \Phi_P / \tau_P$, $k_{nrf} = (1 - \Phi_F - \Phi_P) / \tau_F$, $k_{nrp} = (1 - \Phi_P) / \tau_P$, $k_{ISC} = \Phi_P / \tau_F$.

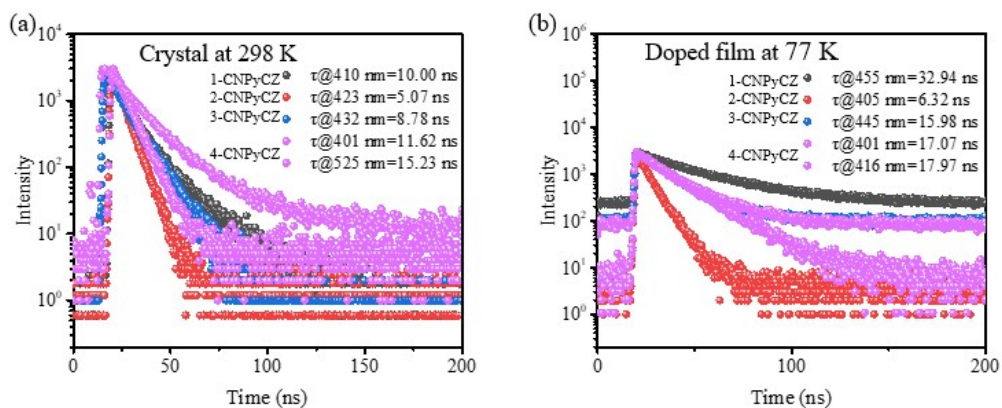


Figure S19. Fluorescence decay curves of 1-CNPyCZ, 2-CNPyCZ, 3-CNPyCZ and 4-CNPyCZ crystalline powder at different states: (a) crystal at 298 K and (b) doped film at 77 K.

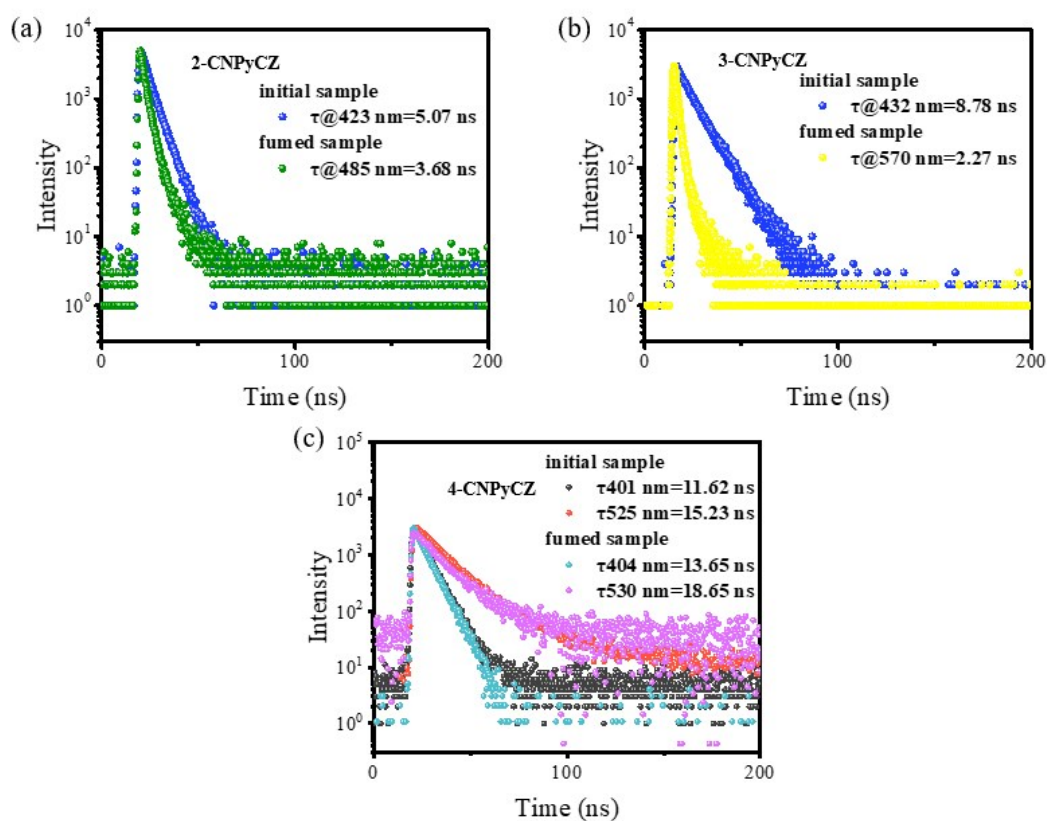


Figure S20. Fluorescence decay curves of (a) 2-CNPyCZ, (b) 3-CNPyCZ and (c) 4-CNPyCZ crystalline powder before and after fuming.

9. Unit cell in the single crystal of 1-CNPyCZ, 2-CNPyCZ and 4-CNPyCZ

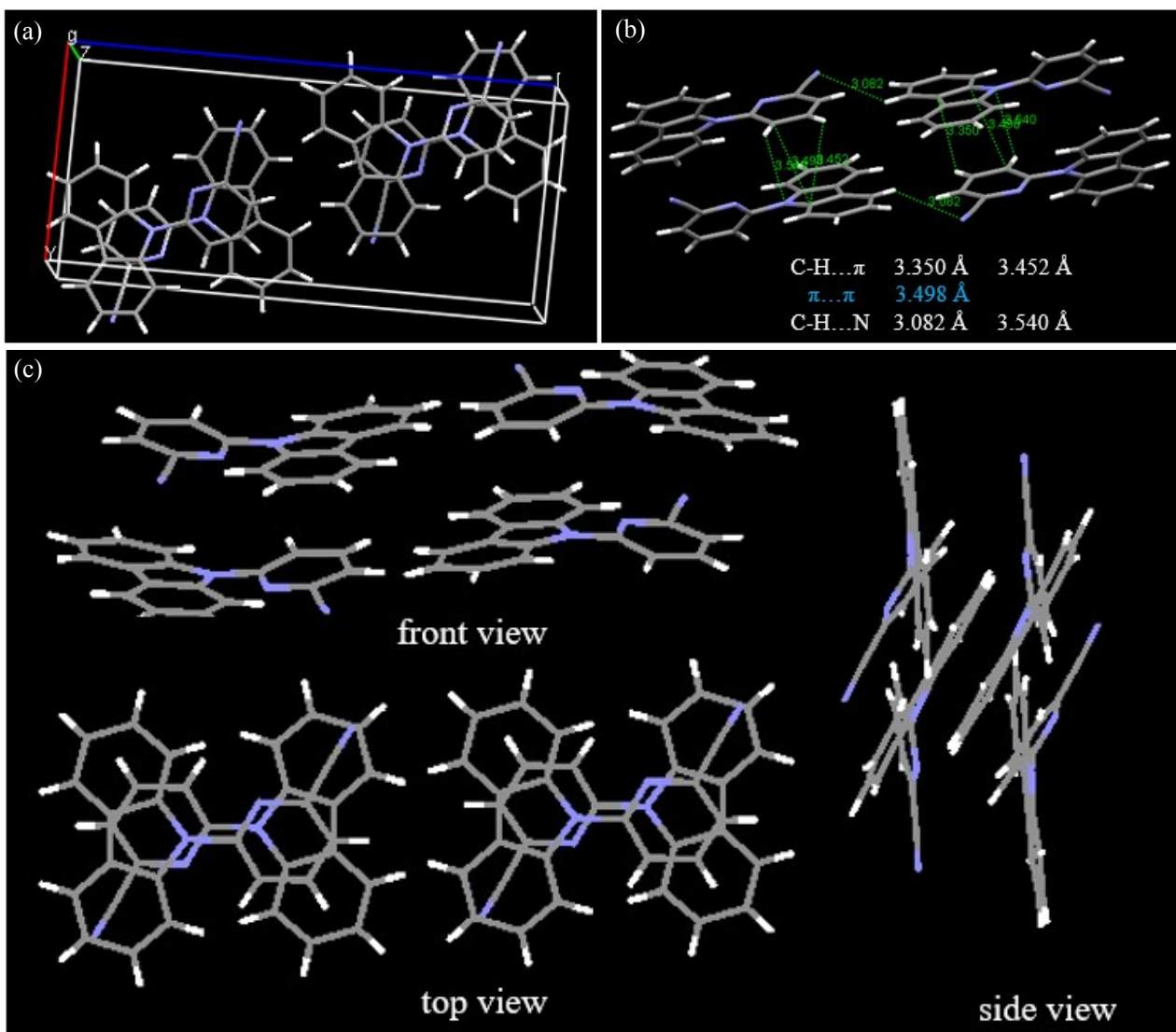


Figure S21. (a) The steric unit cell of 1-CNPyCZ; (b) the intermolecular interactions between adjacent molecules; (c) Packing modes of the crystals for 1-CNPyCZ.

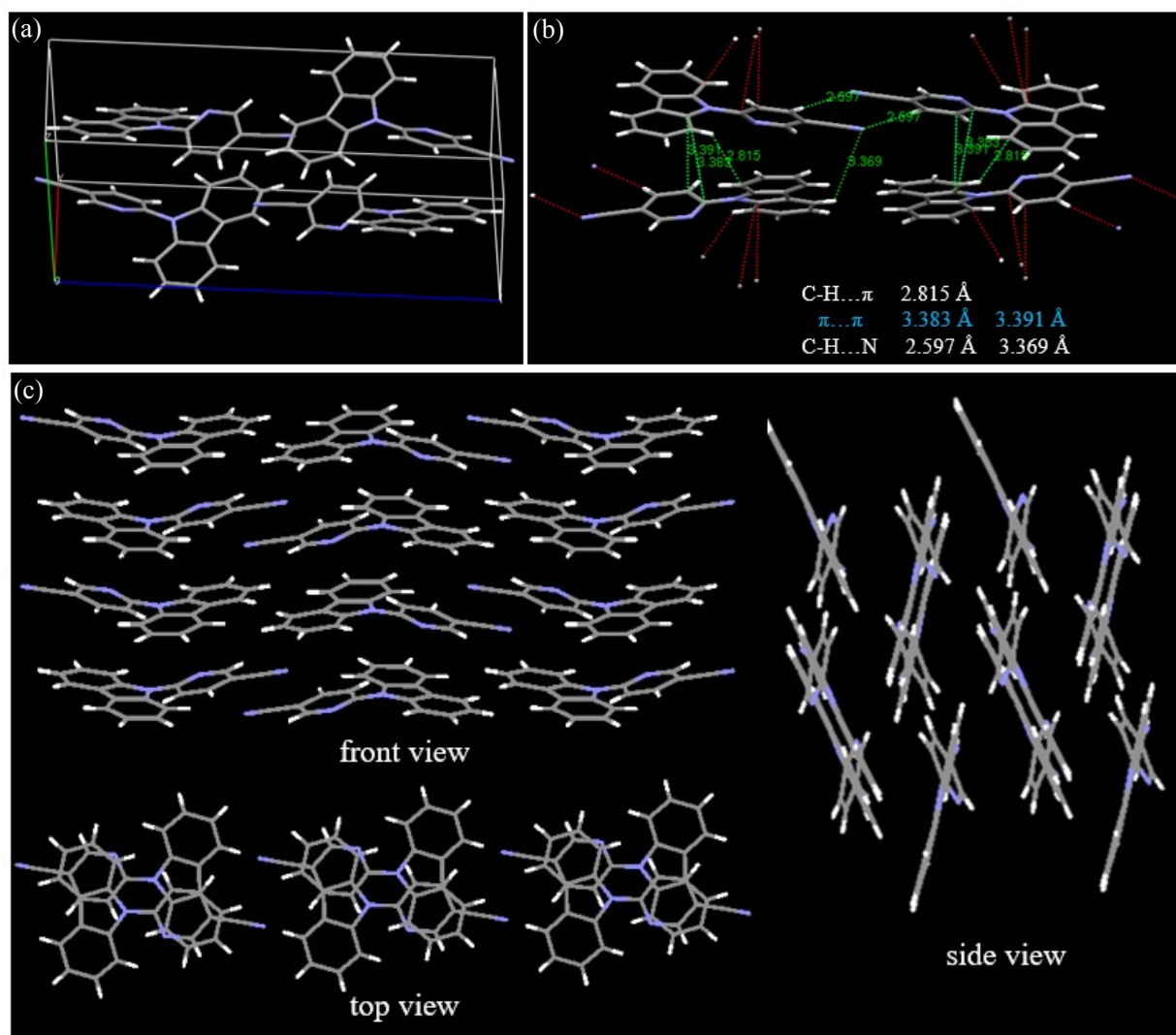


Figure S22. (a) The steric unit cell of **2-CNPyCZ**; (b) the intermolecular interactions between adjacent molecules; (c) Packing modes of the crystals for **2-CNPyCZ**.

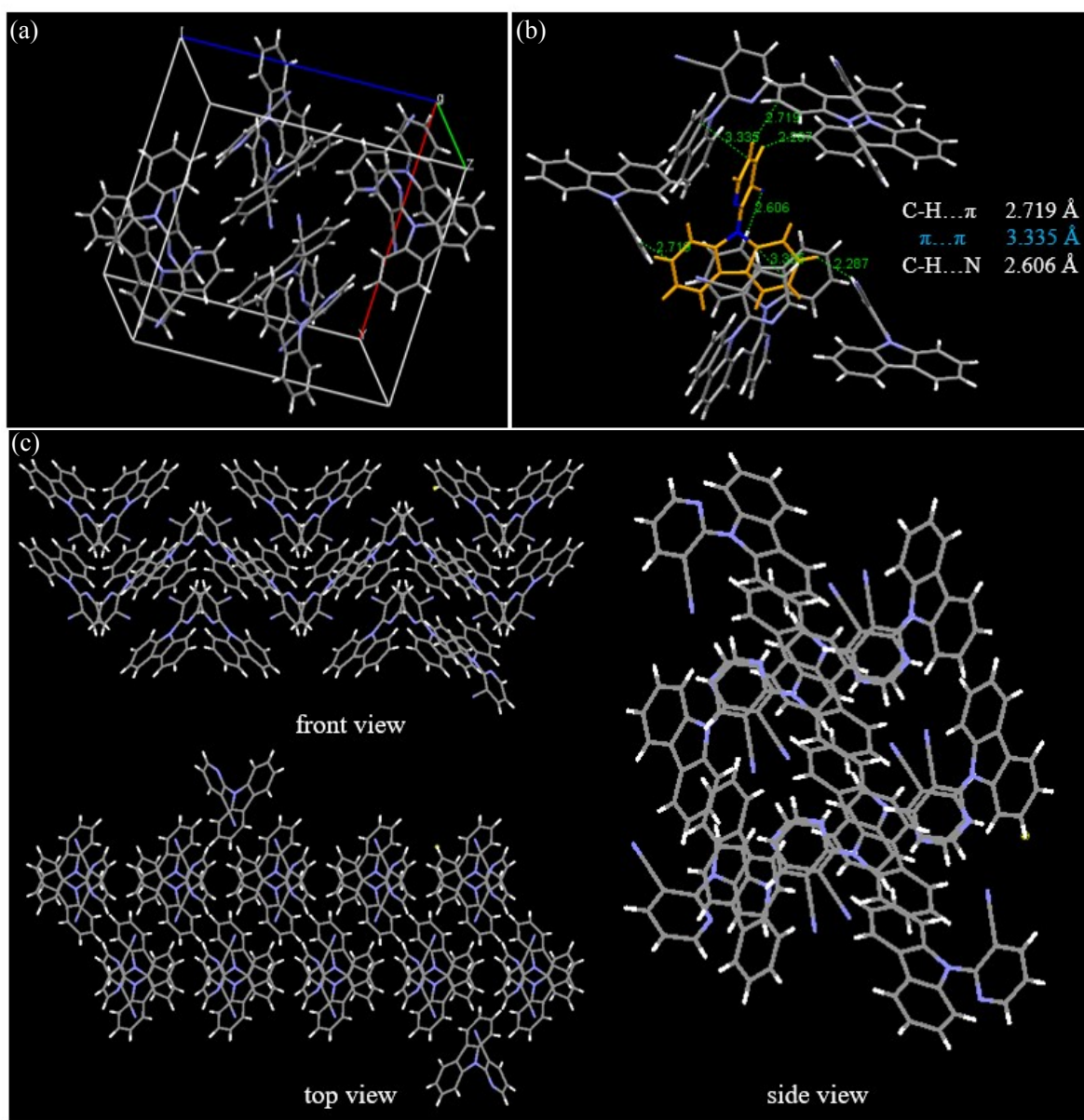


Figure S23. (a) The steric unit cell of **4-CNPycZ**; (b) the intermolecular interactions between adjacent molecules; (c) Packing modes of the crystals for **4-CNPycZ**.

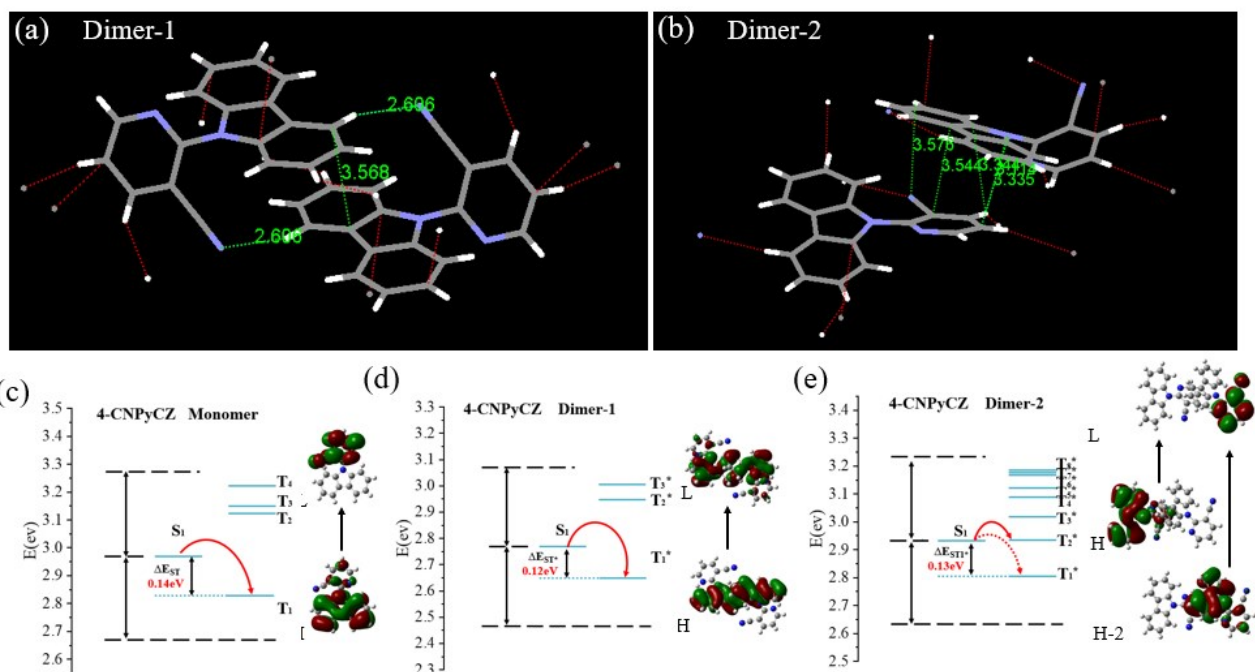


Figure S24. Crystal structures of 4-CNPyCZ (a, b), (a) is the Dimer-1 and (b) is the Dimer-2. Diagrams of the TD-DFT calculated energy levels and possible ISC channels of 4-CNPyCZ monomer (c), dimer-1 (d), dimer-2 (e) at the singlet (S_1) and triplet (T_n) states. H and L represent the HOMO and the LUMO, respectively. The red solid and dashed arrows represent major and minor ISC channels, respectively; the black dashed line represents energy levels between $S_1 \pm 0.3$ eV.

10. XRD patterns and DSC curves

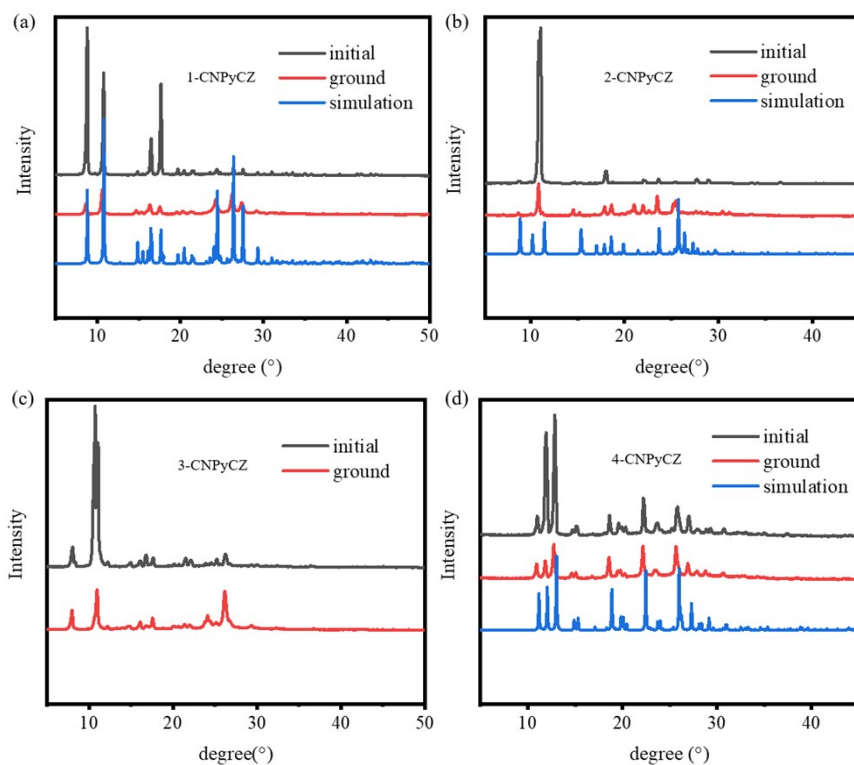


Figure S25. XRD patterns of (a) 1-CNPyCZ, (b) 2-CNPyCZ, (c) 3-CNPyCZ and (d) 4-CNPyCZ: initial powder, ground powder and the simulated patterns based on the single crystal data.

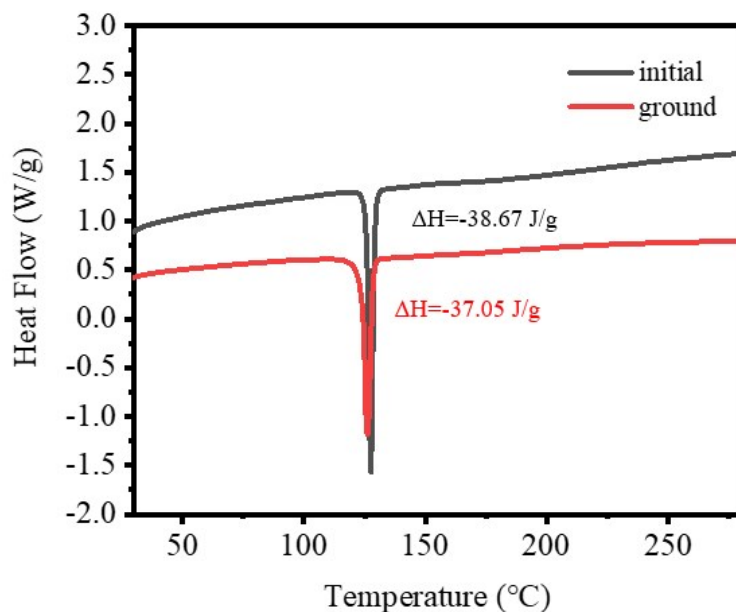


Figure S26. DSC curves of 4-CNPyCZ powder.

11. TD-DFT results

Table S4. TD-DFT calculated singlet and triplet excited states transition configurations of 4-CNPyCZ.

Excited State	Energy (eV)	Transition configuration (%)
Monomer		
T1	2.8276	H-4→L(2.8%), H→L(93.2%), H→L+1(2.1%)
S1	2.9708	H→L(99.3%)
T2	3.1221	H→L(2.9%), H-1→L+2(6.9%), H→L+1(78.5%)
T3	3.1492	H-2→L+2(2.5%), H-1→L(19.0%), H-1→L+1(5.8%), H-1→L+2(48.9%), H→L+1(6.9%), H→L+2(3.0%), H→L+4(5.6%)
T4	3.2221	H-1→L(78.9%), H-1→L+2(15.1%)
Dimer 1		
T1	2.6479	H-2→L+1(24.1%), H-1→L+1(4.3%), H→L(67.5%)
S1	2.7686	H-2→L+1(18.5%), H-1→L+1(3.8%), H→L(77.3%)
T2	2.9463	H-3→L(11.9%), H-2→L+1(3.0%), H-1→L+1(80.0%)

T3	3.0054	H-2→L+3(27.7%), H-1→L+3(4.9%), H→L+2(57.8%)
Dimer 2		
T1	2.8066	H-10→L(2.3%), H-2→L(91.7%)
S1	2.9346	H-2→L(28.2%), H→L(69.4%)
T2	2.9351	H→L(93.0%), H→L+2(4.5%)
T3	3.0170	H-6→L+2(4.1%), H→L(5.1%), H→L+1(2.1%), H→L+2(76.5%), H→L+3(5.4%)
T4	3.0875	H-3→L+4(6.7%), H-2→L(2.5%), H-2→L+1(77.2%)
T5	3.1211	H-3→L(24.5%), H-3→L+1(4.6%), H-3→L+2(4.4%), H-3→L+4(36.8%), H-2→L+1(6.4%), H-2→L+4(4.4%), H-2→L+7(3.1%)
T6	3.1691	H-4→L+5(3.7%), H-1→L+5(70.8%), H→L+5(2.7%)
T7	3.1789	H-3→L(2.4%), H-1→L(95.7%)
T8	3.1839	H-3→L(68.6%), H-3→L+4(15.7%), H-1→L(3.4%)

References

1. J.-A. Li, J. Zhou, Z. Mao, Z. Xie, Z. Yang, B. Xu, C. Liu, X. Chen, D. Ren, H. Pan, G. Shi, Y. Zhang and Z. Chi, *Angew. Chem. Int. Ed.*, 2018, **57**, 6449-6453.
2. Z. An, C. Zheng, Y. Tao, R. Chen, H. Shi, T. Chen, Z. Wang, H. Li, R. Deng, X. Liu and W. Huang, *Nature Materials*, 2015, **14**, 685-690.
3. S. Xu, T. Liu, Y. Mu, Y.-F. Wang, Z. Chi, C.-C. Lo, S. Liu, Y. Zhang, A. Lien and J. Xu, *Angew. Chem. Int. Ed.*, 2015, **54**, 874-878.
4. Y. Gong, G. Chen, Q. Peng, W. Z. Yuan, Y. Xie, S. Li, Y. Zhang and B. Z. Tang, *Adv. Mater.*, 2015, **27**, 6195-6201.
5. Z. Mao, Z. Yang, Y. Mu, Y. Zhang, Y.-F. Wang, Z. Chi, C.-C. Lo, S. Liu, A. Lien and J. Xu, *Angew. Chem. Int. Ed.*, 2015, **54**, 6270-6273.

6. B. Xu, Y. Mu, Z. Mao, Z. Xie, H. Wu, Y. Zhang, C. Jin, Z. Chi, S. Liu, J. Xu, Y.-C. Wu, P.-Y. Lu, A. Lien and M. R. Bryce, *Chemical Science*, 2016, **7**, 2201-2206.
7. B. Huang, Z. Li, H. Yang, D. Hu, W. Wu, Y. Feng, Y. Sun, B. Lin and W. Jiang, *J. Mater. Chem. C*, 2017, **5**, 12031-12034.
8. L. Gu, H. Shi, M. Gu, K. Ling, H. Ma, S. Cai, L. Song, C. Ma, H. Li, G. Xing, X. Hang, J. Li, Y. Gao, W. Yao, Z. Shuai, Z. An, X. Liu and W. Huang, *Angewandte Chemie International Edition*, 2018, **57**, 8425-8431.
9. L. Huang, J. Liu, L. Liu, Q. Yang, Z. Ma and X. Jia, *Dyes and Pigments*, 2020, **173**, 107963.
10. Z. He, H. Gao, S. Zhang, S. Zheng, Y. Wang, Z. Zhao, D. Ding, B. Yang, Y. Zhang and W. Z. Yuan, *Adv. Mater.*, 2019, **31**, 1807222.